Migrating Shear Bands in Shaken Granular Matter

Jonathan E. Kollmer, Tara Shreve, Joelle Claussen, Stefan Gerth, Michael Salamon, Norman Uhlmann, Matthias Schröter, Thorsten Pöschel

Migrating Shear Bands in Shaken Granular Matter

Jonathan E. Kollmer,[1,2,3,*] Tara Shreve,[1,4] Joelle Claussen,[5] Stefan Gerth,[5] Michael Salamon,[5] Norman Uhlmann,[5] Matthias Schröter,[1,6,†] and Thorsten Pöschel[1]

[1]*Institute for Multiscale Simulation of Particulate Systems, Cauerstraße 3, 91058 Erlangen, Germany*
[2]*Department of Physics, 2401 Stinson Drive, North Carolina State University, Raleigh, North Carolina 27695, USA*
[3]*Experimentelle Astrophysik, Universitt Duisburg-Essen, Lotharstraße 1-21, 47057 Duisburg, Germany*
[4]*Université de Paris, Institut de physique du globe de Paris, CNRS, F-75005 Paris, France*
[5]*Fraunhofer-Entwicklungszentrum Röntgentechnik, Flugplatzstraße 75, 90768 Fürth, Germany*
[6]*Max Planck Institute for Dynamics and Self-Organization, 37077 Göttingen, Germany*

(Received 18 February 2020; revised 18 June 2020; accepted 25 June 2020; published 21 July 2020)

When dense granular matter is sheared, the strain is often localized in shear bands. After some initial transient these shear bands become stationary. Here, we introduce a setup that periodically creates horizontally aligned shear bands which then migrate upward through the sample. Using x-ray radiography we demonstrate that this effect is caused by dilatancy, the reduction in volume fraction occurring in sheared dense granular media. Further on, we argue that these migrating shear bands are responsible for the previously reported periodic inflating and collapsing of the material.

DOI: 10.1103/PhysRevLett.125.048001

Introduction.—Granular materials such as sand, sugar, soil, or snow are ubiquitous in our daily lives. However, their dynamics, i.e., their flow behavior when poured into a container or their tendency to segregate when agitated, is often only poorly understood. This problem originates from the macroscopic size of the individual particles: The potential energy involved in lifting a grain its own diameter is many orders of magnitude larger than the energy provided by Brownian motion. Therefore, any granular dynamics requires external driving. Additionally, individual, macroscopic grains interact dissipatively, thus, any continuous dynamics requires also continuous driving. As a consequence, the dynamics of the granular sample depends on the specific type of driving, complicating the search for the potentially underlying unifying principles.

In this Letter, we present an experiment that uses horizontal shaking as the driving mechanism: Granular material is confined in a rectangular container and shaken horizontally and sinusoidally with constant amplitude A and frequency f. The agitation by horizontal shaking displays an interesting phenomenology which combines two different types of response: Above a certain threshold acceleration [1–5], the upper part of the sample starts sloshing in the container while the lower part stays solidlike. In between these two parts then a horizontal *shear band* forms [6,7]. Additionally the upper, sloshing, part develops two counterrotating *convection rolls*. The driving mechanism for these rolls are downhill flows at the two end gaps created by the sloshing motion [2–4,6–12]. Rough boundaries, stronger excitation, different container shapes, or the absence of friction can create even more complex convection patterns [10–14]. Moreover, horizontal shaking has proven itself as a fertile model system for compaction [12,15,16], transport [17], pattern formation [18–21], crystallization of monodisperse spheres [22,23], and segregation of bidisperse samples [19,20,24–26].

Understanding shear bands and where they will emerge is an active area of research [27]. For slow granular flows a variational model minimizing the total dissipation is successful in predicting the location of the shear band, especially in samples composed of materials with different friction coefficients [28–31]. Alternative approaches explain the emergence of shear bands from the dynamics of force chain networks [32,33]. Recently, it has been discovered that there also can be precursor microbands which are not aligned with the final shear bands [34].

Inside a shear band the volume fraction ϕ decreases to a characteristic volume fraction ϕ_{SB} [35–38]. This is due to dilatancy [39–42], the fact that dense granular materials need to expand when sheared. ϕ_{SB} depends on the shear rate [36,43] and the friction coefficient [37].

In this Letter, we study the dynamics of the horizontal shear band forming between the upper sloshing and the lower stationary part [6,7] of a horizontally shaken granular system. We report here for the first time (a) the existence of multiple shear bands in this system and (b) that some of these bands are not stationary but migrate upward on a timescale much slower than the driving frequency. Such a migration of shear bands has to our knowledge not been identified in any other granular system with periodic driving. Using x-ray radiography we show that these dynamics correspond to dilatancy waves. Moreover, these dilatancy waves explain the recurrent alternation between slow inflation and fast collapse of the sample surface which has been reported previously [44].

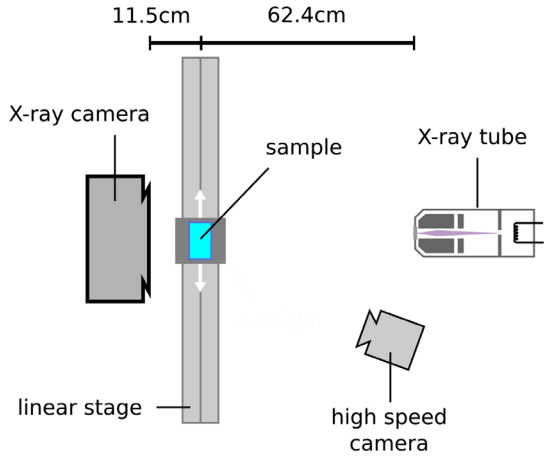

FIG. 1. Top view of the experimental setup. The sample box moves horizontally on a linear stage and is driven by a stepper motor via a gear belt. The dynamics in the sample is observed simultaneously with x rays in transmission and with visible light at the sidewall of the sample box.

Experimental setup.—The granular material used in all experiments is construction sand with a mean grain diameter of (265 ± 70) μm (measured with a Retsch Camsizer), and a density of (2.6699 ± 0.0003) g/cm^3 (measured with an AccuPyc II 1340 helium pycnometer). 270 g of this sand is filled in a rectangular sample box made from transparent, 4 mm thick polycarbonate plates. The inner dimensions of the sample box are $100 \times 50 \times 50$ mm^3.

The sample box is mounted on a platform which moves horizontally on a linear bearing driven by a computer controlled stepper motor. The platform performs sinusoidal oscillations of frequency $f = 18$ Hz and amplitude $A = 1.5$ mm, resulting in a horizontal acceleration amplitude $\Gamma = 4\pi^2 A f^2 = 2g$. For a schematic drawing of the setup see Fig. 1.

In order to study the fast granular dynamic in the bulk of the shaken sample, we use x-ray radiograms such as the one shown in Fig. 2. X rays were created with a Comet 225-HP tube at 160 kV and 6.2 mA using a focal spot of 1 mm diameter at the tungsten target. The x-ray detector is a Fraunhofer EZRT X-Eye2020 with 300 μm CsI scintillator; image size is 500 by 500 pixels (binned) with a pixel size of 400 μm. Combined with a geometric magnification of 1.18 this corresponds to an imaging scale of 338 μm/pixel. Images were taken with an exposure time of 5 ms and phase locked with the driving. The necessary trigger signal was obtained from a Hall-effect-based position encoder which measured the position of the sample container with spatial resolution of 20 μm at a sampling rate of 10 kHz. Additionally, the sidewall of the sample box was imaged with visible light using a high-speed camera at 500 frames per second. These images allow a simultaneous measurement of the velocity field of the outer layer of grains using particle image velocimetry (PIV) and are discussed in Sec. IV of the Supplemental Material [45].

Computing volume fractions from x-ray images.—We quantify the spatiotemporal changes of the volume fraction ϕ using the intensity I of the transmitted x rays. If a sample is imaged with *monoenergetic* x rays, the transmitted intensity is given by the Lambert-Beer law: $I = I_0 e^{-\mu \Delta x}$, where I_0 is the incident intensity, Δx the thickness of the sample, and μ the absorption coefficient of the material. In a granular sample this relationship can be used to measure the length l_s that the beam has traveled inside the sample material itself, as opposed to the interstitial space which is typically filled with air (with a negligible value of μ). From l_s we can then compute the volume fraction ϕ, averaged along the path of the beam: $\phi(I) = \{[l_s(I)]/l_{\mathrm{box}}\}$ where l_{box} is the inner length of the box in the beam direction (5 cm in our experiment). This method has previously been

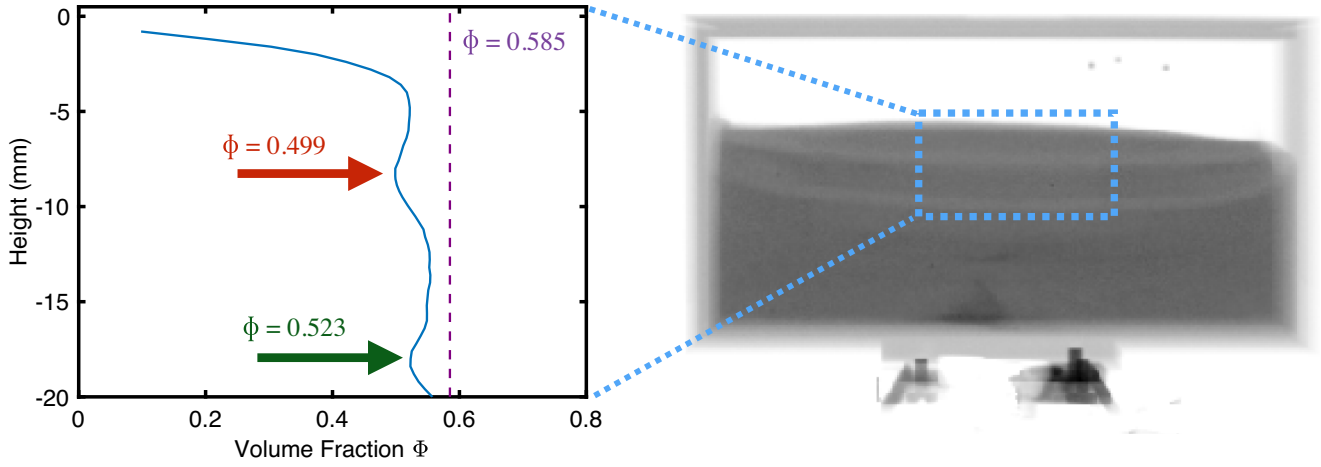

FIG. 2. X-ray radiograms can be used to measure the volume fraction averaged along the path of the x rays. The right panel shows a radiogram of sand shaken sinusoidally at 18 Hz. To track the position of the low density zone, the image intensity is averaged horizontally in the area indicated by the dashed line. From this average intensity follows the average volume fraction shown in the left panel. The arrows indicate the position of the shear bands.

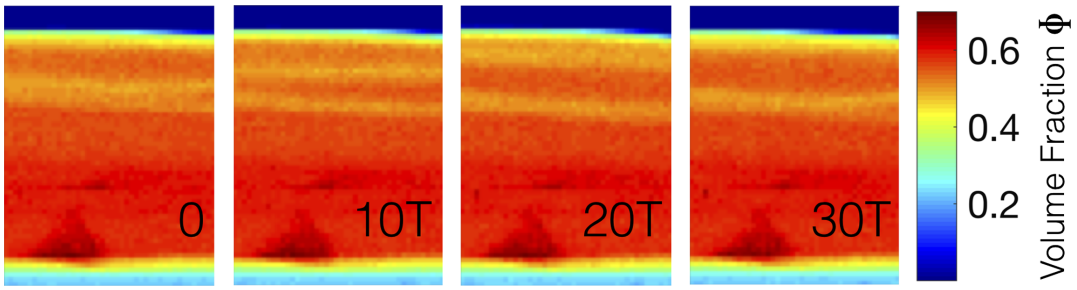

FIG. 3. Radiograms of the center part of the sample, shaken at $f = 18$ Hz. Images taken after an integer number of oscillations periods T show an approximately stationary stripe of lower density split into two with the upper stripe then moving upward. Please see the Supplemental Material [45] for an animated version of the radiograms.

used to study qualitatively the density variations in flowing sand [46–48], dilatancy during fast shear [36], the subsurface swimming of sandfish lizards [49], effective temperatures in vibrated samples [50], concentration maps in suspensions [51,52], compaction [53], and the formation of a granular jet after a sphere impact into a granular medium [54,55].

If the experimental setup is based on an x-ray tube, i.e., uses a *polyenergetic* Bremsstrahlung spectrum, a quantitative analysis has to take the so-called beam hardening effect into account: Because the attenuation coefficient μ is a function of the energy E of the photons, the spectral composition of the beam will change with depth inside the sample material. As a consequence, the Lambert-Beer law is oversimplified and we need to replace the constant μ with an effective $\mu_{\mathrm{eff}}(l_s)$ which depends on the thickness of the sample material. Because the functional form of $\mu_{\mathrm{eff}}(l_s)$ does also depend on the exact shape of the x-ray spectrum and on the energy dependence of the sensitivity of the camera, $\mu_{\mathrm{eff}}(l_s)$ cannot be derived mathematically but has to be determined from independent calibration measurements [56]. Section I of the Supplemental Material describes how to compute the volume fractions shown, e.g., in the abscissa of Fig. 2.

Migrating low density bands.—The x-ray radiograms shown in Fig. 3 reveal that the sample responds to the onset of the shaking with the formation of horizontal stripes of lower density. These stripes span the whole width of the sample cell as shown in the movies in the Supplemental Material [45]. As these images are synchronized with the shaking frequency, they do not display the fast sloshing motion (due to the horizontal driving) in the upper part of the sample. The stripes always start to form at the same height, and based on [28] we can speculate that this height is determined by the interplay of sloshing velocity and local pressure. Further, the shear gradient at the boundary between the sloshing and the static part has to become steep enough that dilatancy starts to play a role [7].

The spatiotemporal dynamics of these low density bands is quite rich. In the vicinity of the left and right sidewall the bands are curved upward, additionally even more inclined, transient bands form. This more complicated dynamics might be attributed to the strong convection rolls present in that area.

In the center part of the box, horizontal stripes form and then split into two. The upper stripes always move toward the upper surface, where they vanish. The lower stripes either travel slowly downward or stay constant in height; but in both cases they continue to spawn upward traveling stripes. All stripe migration occurs on timescales much slower than the driving frequency and is reset in apparently irregular time intervals. Such intermittent timescales are a frequent phenomenon in sheared granular matter [57]. Figure 3 illustrates this dynamics. The formation and migration of stripes occurs over a range of driving frequencies; in the Supplemental Material we show the equivalent of Fig. 3 measured at 25 Hz. As shaking at 25 Hz leads to a more complex convective motion we will focus on the 18 Hz case here.

In order to quantify the upward migration of the upper low density bands, we track the height h of the local minimum in the $\phi(h)$ curves, as illustrated in Fig. 2. Figure 4 shows that the upper diluted zones migrate within 2 s and at an approximately constant velocity to the top of the sample where they vanish. At about the same time new bands respawn from the stationary stripe.

From the image intensity we determine the average volume fraction inside the migrating, diluted zone (see Fig. 2 of Supplemental Material [45] for details) as $\phi_{\mathrm{SB}} = 0.486 \pm 0.006$ and in the bulk below the bands as

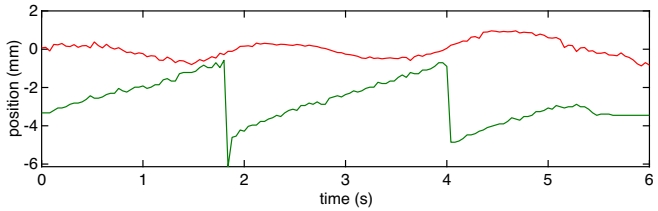

FIG. 4. Evolution of the height of the sample surface (red) and the position of the density minimum (green) during 108 shaking cycles ($f = 18$ Hz). As the radiograms are phase synchronized, all heights are measured once per shaking cycle and are relative to the mean surface height.

$\phi_{\mathrm{bulk}} = 0.585 \pm 0.009$. Figure 2 of the Supplemental Material [45] contains a more detailed overview of ϕ in various locations of the system. Based on these results, we suggest that the mechanism driving the upward migration of the stripes is actually gravity: The fabric within the diluted band (or shear band as we will show in the next section) is not capable of supporting the weight of the layer of grains directly above it. These will move downward into the available void space, in this way moving the diluted zone upward.

Shear bands.—It is already known that the particles in the upper part of a horizontally shaken sample perform a sloshing motion while the particles in the bottom part stay at rest in the reference frame of the box. However, with the exception of PIV measurements in Refs. [6,7], the resulting shear band had previously not been the focus of the attention. This is at least in part due to the fact that most experiments had used imaging which was phase locked with the driving, thereby effectively freezing the sloshing motion. The division of the bed into a stationary and a sloshing part is also valid in our experiments. This can be seen from the PIV images taken with the high speed camera and shown in Sec. IV of the Supplemental Material [45].

In order to prove that the migrating low density bands shown in Fig. 3 are actually shear bands, or more precisely bands with a strong vertical gradient of the horizontal velocity, we need to measure simultaneously both the velocity within the sample (not only at the sidewalls as with the PIV) and the spatiotemporal evolution of ϕ. Therefore, we add a small amount of steel spheres as tracers to the sand. Their diameter of 2 mm was determined empirically: They are large enough that the void filling mechanism driving them upward [58] is approximately compensating their tendency to sink to the bottom due to their higher material density compared to sand. Additionally, they provide a good contrast in the x-ray radiograms.

Each image in Fig. 5 shows the superposition of two radiograms that were recorded half a shaking period apart, that is in opposing phases of the sloshing motion. In order to visualize the motion, the two radiograms have been converted to complementary color channels before combining them. In this way the black dots in the combined image indicate tracers that did not move noticeably between frames and the pairs of blue and red dots indicate the position of a moving tracer at time $t = 0$ and $t = T/2$, respectively.

The main message of Fig. 5 is that the two low density bands each correspond to a significant change in the horizontal velocity of the particles, i.e., regions of high shear. Since we can identify the diluted bands as shear bands, their reduced volume fraction ϕ_{SB} can directly be attributed to dilatancy.

Traveling shear bands explain periodic height changes.—It has been previously reported that the upper surface of a horizontally shaken sample rises and sinks periodically with an amplitude of about 5% of the total filling height [44]. The frequency of this periodic expansion and contraction is approximately 0.4 Hz, independent of the driving frequency. This periodic height change is also present in our experiment: Fig. 4 displays in red the periodic change of the surface height. Plotting it alongside the position of the migrating shear zone suggests that these two effects are correlated. The expansion would then be due to the formation of the dilute shear bands, the height reduction due to their disappearance.

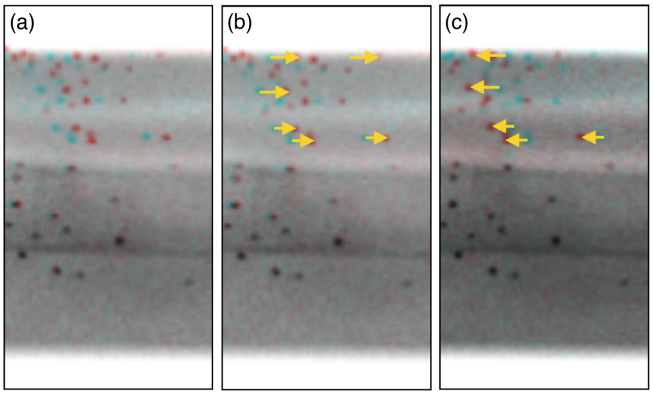

FIG. 5. By adding stainless steel tracers (diameter 2 mm) we can determine local velocities inside the bulk of the material and show that the low density zones coincide with regions where the magnitude of horizontal component of the velocity abruptly changes, that is, regions of high shear. Images (a) to (c) are each superpositions of two radiograms taken half a shaking period apart. Pairs of red and blue dots correspond to moving tracer particles, black dots are tracer particles at rest within the comoving frame of the box. Image (b) indicates the tracer particle motion visible in (a) by yellow arrows. Image (c) shows the motion half a period later.

Conclusions.—Granular matter in a horizontally shaken container develops horizontal shear bands separating an upper part, which is in a sloshing motion, from a lower, stationary part. Because of the effect of dilatancy, these shear bands have a lower volume fraction then the material surrounding them. Because particles above the shear band are not sufficiently mechanically supported they fall into the more dilute area below, resulting in an upward motion of the band. Such traveling shear bands in an otherwise stationary situation are a new granular phenomenon. Because horizontal agitation is a common process in the handling and transport of granular media, this effect can be expected to be also relevant in a variety of industrial applications.

We acknowledge Rachel Derby and Achim Sack for technical assistance. J. E. K., T. P., and M. S. thank the German Science Foundation (DFG) for funding through the Cluster of Excellence Engineering of Advanced Materials. T. S. thanks the German Academic Exchange Service (DAAD) for funding through the RISE Program in 2015.

*jonathan.kollmer@uni-due.de
†matthias.schroeter@ds.mpg.de

[1] G. H. Ristow, G. Straßburger, and I. Rehberg, Phys. Rev. Lett. **79**, 833 (1997).
[2] S. G. K. Tennakoon, L. Kondic, and R. P. Behringer, Europhys. Lett. **45**, 470 (1999).
[3] G. Metcalfe, S. G. K. Tennakoon, L. Kondic, D. G. Schaeffer, and R. P. Behringer, Phys. Rev. E **65**, 031302 (2002).
[4] S. Aumaitre, C. Puls, J. N. McElwaine, and J. P. Gollub, Phys. Rev. E **75**, 061307 (2007).
[5] M. Heckel, A. Sack, J. E. Kollmer, and T. Pöschel, Phys. Rev. E **91**, 062213 (2015).
[6] M. Medved, H. M. Jaeger, and S. R. Nagel, Europhys. Lett. **52**, 66 (2000).
[7] M. Medved, Phys. Rev. E **65**, 021305 (2002).
[8] K. Liffman, G. Metcalfe, and P. Cleary, Phys. Rev. Lett. **79**, 4574 (1997).
[9] C. Salueña, T. Pöschel, and S. E. Esipov, Phys. Rev. E **59**, 4422 (1999).
[10] M. Medved, D. Dawson, H. M. Jaeger, and S. R. Nagel, Chaos **9**, 691 (1999).
[11] C. Salueña and T. Pöschel, Eur. Phys. J. E **1**, 55 (2000).
[12] S. Nadler, O. Bonnefoy, J.-M. Chaix, G. Thomas, and J.-L. Gelet, Eur. Phys. J. E **34**, 66 (2011).
[13] S.-S. Hsiau, M.-Y. Ou, and C.-H. Tai, Adv. Powder Technol. **13**, 167 (2002).
[14] A. Raihane, O. Bonnefoy, J. L. Gelet, J. M. Chaix, and G. Thomas, Powder Technol. **190**, 252 (2009).
[15] A. Raihane, O. Bonnefoy, J. M. Chaix, J. L. Gelet, and G. Thomas, Powder Technol. **208**, 289 (2011).
[16] L. Olmos, J.-M. Chaix, S. Nadler, O. Bonnefoy, J.-L. Gelet, and G. Thomas, Granular Matter **18**, 61 (2016).
[17] S. Mobarakabadi, E. N. Oskoee, M. Schröter, and M. Habibi, Phys. Rev. E **88**, 042201 (2013).
[18] G. Straßburger, A. Betat, M. A. Scherer, and I. Rehberg, in *Workshop on Traffic and Granular Flow*, edited by D. E. Wolf, M. Schreckenberg, and A. Bachem (World Scientific, Singapore, 1995), pp. 329–334.
[19] M. Pica Ciamarra, A. Coniglio, and M. Nicodemi, Phys. Rev. Lett. **97**, 038001 (2006).
[20] M. Pica Ciamarra, A. Coniglio, and M. Nicodemi, Eur. Phys. J. E **22**, 227 (2007).
[21] D. Krengel, S. Strobl, A. Sack, M. Heckel, and T. Pöschel, Granular Matter **15**, 377 (2013).
[22] O. Pouliquen, M. Nicolas, and P. D. Weidman, Phys. Rev. Lett. **79**, 3640 (1997).
[23] G. Straßburger and I. Rehberg, Phys. Rev. E **62**, 2517 (2000).
[24] P. M. Reis and T. Mullin, Phys. Rev. Lett. **89**, 244301 (2002).
[25] P. M. Reis, T. Sykes, and T. Mullin, Phys. Rev. E **74**, 051306 (2006).
[26] C. Lozano, I. Zuriguel, A. Garcimartín, and T. Mullin, Phys. Rev. Lett. **114**, 178002 (2015).
[27] P. Schall and M. v. Hecke, Annu. Rev. Fluid Mech. **42**, 67 (2010).
[28] T. Unger, Phys. Rev. Lett. **98**, 018301 (2007).
[29] T. Börzsönyi, T. Unger, and B. Szabó, Phys. Rev. E **80**, 060302(R) (2009).
[30] T. Börzsönyi, T. Unger, B. Szabó, S. Wegner, F. Angenstein, and R. Stannarius, Soft Matter **7**, 8330 (2011).
[31] R. Moosavi, M. Maleki, M. R. Shaebani, J. C. Ruiz-Surez, and E. Clément, Europhys. Lett. **107**, 34006 (2014).
[32] K. Iwashita and M. Oda, Powder Technol. **109**, 192 (2000).
[33] D. M. Walker and A. Tordesillas, Phys. Rev. E **85**, 011304 (2012).
[34] A. Le Bouil, A. Amon, S. McNamara, and J. Crassous, Phys. Rev. Lett. **112**, 246001 (2014).
[35] F. Radjaï and S. Roux, in *The Physics of Granular Media*, edited by H. Hinrichsen and D. E. Wolf (Wiley-VCH, Weinheim, 2004), pp. 165–187.
[36] A. J. Kabla and T. J. Senden, Phys. Rev. Lett. **102**, 228301 (2009).
[37] S. Fazekas, J. Török, and J. Kertész, Phys. Rev. E **75**, 011302 (2007).
[38] K. Sakaie, D. Fenistein, T. J. Carroll, M. van Hecke, and P. Umbanhowar, Europhys. Lett. **84**, 38001 (2008).
[39] O. Reynolds, Philos. Mag. **20**, 469 (1885).
[40] N. P. Kruyt and L. Rothenburg, J. Stat. Mech. (2006) P07021.
[41] B. Andreotti, Y. Forterre, and O. Pouliquen, *Granular Media* (Cambridge University Press, Cambridge, England, 2013).
[42] B. P. Tighe, Granular Matter **16**, 203 (2014).
[43] A. Ries, L. Brendel, and D. E. Wolf, Comput. Part. Mech. 1 **3**, 303 (2016).
[44] T. Pöschel, D. E. Rosenkranz, and J. A. C. Gallas, Phys. Rev. E **85**, 031307 (2012).
[45] See Supplemental Material at http://link.aps.org/supplemental/10.1103/PhysRevLett.125.048001 for more details, including movies that consist of phase-locked radiograms capturing the whole width of the sample cells and displaying the evolution of the volume fraction in color code, similar to Fig. 3. Shaking frequencies are 18 and 25 Hz.
[46] R. L. Michalowski, Powder Technol. **39**, 29 (1984).
[47] G. W. Baxter, R. P. Behringer, T. Fagert, and G. A. Johnson, Phys. Rev. Lett. **62**, 2825 (1989).
[48] L. A. Fullard, C. E. Davies, G. Lube, A. C. Neather, E. C. P. Breard, and B. J. Shepherd, Granular Matter **19**, 6 (2017).
[49] R. D. Maladen, Y. Ding, C. Li, and D. I. Goldman, Science **325**, 314 (2009).
[50] Y. Cao, X. Zhang, B. Kou, X. Li, X. Xiao, K. Fezzaa, and Y. Wang, Soft Matter **10**, 5398 (2014).
[51] M. Gholami, A. Rashedi, N. Lenoir, D. Hautemayou, G. Ovarlez, and S. Hormozi, J. Rheol. **62**, 955 (2018).
[52] B. Saint-Michel, S. Manneville, S. Meeker, G. Ovarlez, and H. Bodiguel, Phys. Fluids **31**, 103301 (2019).
[53] P. Ribière, P. Richard, P. Philippe, D. Bideau, and R. Delannay, Eur. Phys. J. E **22**, 249 (2007).
[54] J. R. Royer, E. I. Corwin, A. Flior, M.-L. Cordero, M. L. Rivers, P. J. Eng, and H. M. Jaeger, Nat. Phys. **1**, 164 (2005).
[55] T. Homan, R. Mudde, D. Lohse, and D. van der Meer, J. Fluid Mech. **777**, 690 (2015).
[56] M. Baur, N. Uhlmann, T. Pöschel, and M. Schröter, Rev. Sci. Instrum. **90**, 025108 (2019).
[57] K. A. Dahmen, Y. Ben-Zion, and J. T. Uhl, Nat. Phys. **7**, 554 (2011).
[58] M. Schröter, S. Ulrich, J. Kreft, J. B. Swift, and H. L. Swinney, Phys. Rev. E **74**, 011307 (2006).